Direct damage controlled seismic design of plane steel degrading frames

G. S. Kamaris[1], G. D. Hatzigeorgiou[2,*] and D. E. Beskos[3,4]

[1] School of Engineering, University of Warwick, Coventry CV4 7AL, United Kingdom
[2] Engineering Project Management MSc Program, Hellenic Open University, Patras, Greece.
[3] Department of Civil Engineering, University of Patras, Patras, Greece
[4] Office of Theoretical and Applied Mechanics, Academy of Athens, Athens, Greece

ABSTRACT

A new method for seismic design of plane steel moment resisting framed structures is developed. This method is able to control damage at all levels of performance in a direct manner. More specifically, the method: a) can determine damage in any member or the whole of a designed structure under any given seismic load, b) can dimension a structure for a given seismic load and desired level of damage and c) can determine the maximum seismic load a designed structure can sustain in order to exhibit a desired level of damage. In order to accomplish these things, an appropriate seismic damage index is used that takes into account the interaction between axial force and bending moment at a section, strength and stiffness degradation as well as low cycle fatigue. Then, damage scales are constructed on the basis of extensive parametric studies involving a large number of frames exhibiting cyclic strength and stiffness degradation and a large number of seismic motions and using the above damage index for damage determination. Some numerical examples are presented to illustrate the proposed method and demonstrate its advantages against other methods of seismic design.

Keywords: Seismic Design; Damage indices; Plane steel frames; Performance levels; Inelastic behavior; Low cycle fatigue

1. INTRODUCTION

In earthquake-resistant design of structures, different design methods have been used in practice or proposed by researchers. Among them, one can mention the force-based design (FBD), the displacement-based design (DBD) and the hybrid force/displacement based design (HFD).

According to the FBD method, which is currently employed by existing seismic codes (e.g., EC8 2008), seismic forces are used as the main design parameters. This approach demands the design of the building against structural failures which might endanger human life on the basis of elastic analysis in conjunction with recommended constant values of the behavior (or strength reduction) factor, q to take approximately into account inelastic effects. Finally, deformations beyond which service requirements are no longer met after the detailing of the structure are checked near the end of the design.

The DBD (Chopra and Goel 2001; Sullivan et al. 2003, Priestley et al. 2007) is a promising design method for seismic structural design. The basic idea here is the direct satisfaction of the serviceability requirements, the most important of which is the limitation of displacements. Thus, the DBD determines first the target displacements, then the appropriate stiffness of the structure and finally the structural and member forces, which lead to the dimensions of structural members. Thus, the displacements play here the fundamental role in design.

* Corresponding author: Assoc. Professor G.D. Hatzigeorgiou, Tel.:+30.2610.367769, email: hatzigeorgiou@eap.gr

The HFD (Karavasilis et al. 2008a,b) is a new seismic design method for steel frames which combines the advantages of the well-known force-based and displacement-based seismic design methods. The main characteristics of this method are: (1) treats both drift and ductility demands as input variables for the initiation of the design process through a behavior factor, *q*, which depends on them and the characteristics of the structure (e.g. the number of stories); (2) makes use of current seismic code approaches as much as possible (e.g., conventional elastic response spectrum analysis and design); and (3) recognizes the influence of the type of the lateral load resisting system.

The performance based design (PBD) (SEAOC 1999; Leelataviwat et al. 1999) introduces a new and general framework in seismic design of structures by defining performance levels and objectives. Thus, three to five structural performance levels are defined and should be achieved for increasing levels of earthquake actions by satisfying performance objectives for every performance level. These performance objectives mainly refer to the damage of a structure, which is quantified through indices, such as the interstory drift ratio (IDR), or the member plastic rotations.

Displacement-based and in general performance-based seismic design methods employ indirectly (through displacements) or directly the concept of damage, usually quantified with the aid of various damage indices (Kamaris et al. 2013; Powell and Allahabadi 1988, Cosenza et al. 1993; Ghobarah et al. 1999). These indices are expressed in terms of deformation, dissipated energy or a combination of deformation and dissipated energy.

Among the works dealing with damage-based seismic design methods one can mention the following representative ones:

i) those of Park et al. (1987) with an explicit tolerable level of damage and of Panyakapo (2008) based on a damage-based capacity-demand method
ii) those of Aschheim (2002) and Safar and Ghobarah (2008) based on yield displacement spectra where damage is considered indirectly
iii) those of Kawashima and Aizawa (1986), Ballio and Castiglioni (1994), Tiwari and Gupta (2000), Kunnath and Chai (2004), Lu and Wei (2008) and Teran-Gilmore and Bahema-Arredondo (2008) based on inelastic spectra obtained with the aid of a damage dependent behavior or strength reduction factor
iv) those of Malhotra (2002), Bozorgnia and Bertero (2004), Panyakapo (2004) and Ghobarah and Safar (2010) employing damage or cyclic demand spectra.

In this paper, the Direct Damage Controlled Design (DDCD) method, a new design method for steel moment resisting framed structures under earthquake excitation, is proposed. The basic advantage of DDCD is the dimensioning of structural members or whole framed structures with damage directly controlled at both local and global levels. In other words, the designer can select a priori the desired level of damage in a structural member or a whole structure and direct his design in order to achieve this preselected level of damage. In addition, the method can determine damage in any member or the whole of a designed structure under any seismic load and can also determine the maximum seismic load a designed structure can sustain in order to exhibit a desired level of damage. The proposed method works with a new seismic damage index recently developed by the authors (Kamaris et al. 2013) and detailed damage scales developed herein through extensive parametric studies involving a large number of frames and seismic motions. The DDCD method controls damage directly and not indirectly through deformation as the DBD or the HFD methods, is more accurate than any of the abovementioned methods and in addition it can be employed in three different ways, i.e., for damage determination, member dimensioning or maximum seismic load determination. However, the proposed method requires nonlinear dynamic analysis, which is usually time consuming.

The method can be considered as a much improved extension from the static to the dynamic case of a design method previously developed by the authors (Hatzigeorgiou and Beskos 2007; Kamaris et al. 2009) for plane concrete / masonry and steel frames, respectively. In Hatzigeorgiou and Beskos (2007) damage was an internal variable in the stress-strain relation for concrete and computed as a function of deformation, while in Kamaris et al. (2009) damage was expressed in the form of a damage index defined for simple elastoplastic behavior without cyclic deterioration in

stiffness and strength as it is presently the case. Furthermore, the present method does not require directly or indirectly special damage-based design spectra and associated damage dependent behavior or strength reduction factors as it is the case with Kawashima and Aizawa (1986), Ballio and Castiglioni (1994), Tiwari and Gupta (2000), Kunnath and Chai (2004), Lu and Wei (2008), Teran-Gilmore and Bahema-Arredondo (2008), Malhotra (2002), Bozorgnia and Bertero (2004), Panyakapo (2004) and Ghobarah and Safar (2010), works in the framework of three damage levels obtained herein through extensive parametric studies, which is not the case with the abovementioned authors and provides all the three aforementioned design options instead of just the first and/or the second design option as it is the case with Kawashima and Aizawa (1986), Ballio and Castiglioni (1994), Tiwari and Gupta (2000), Kunnath and Chai (2004), Lu and Wei (2008), Teran-Gilmore and Bahema-Arredondo (2008), Malhotra (2002), Bozorgnia and Bertero (2004), Panyakapo (2004) and Ghobarah and Safar (2010). To be sure, Abbas and Takewaki (2010) and Abbas (2011) have also considered the aforementioned third design option (determine the seismic load for a desired damage level) separately by employing a completely different approach. The present design method works with a time domain dynamic inelastic analysis, which is a more complicated approach than the ones based on inelastic spectrum analysis. However, unlike methods based on spectrum analysis, takes into account material and geometric nonlinearities directly and in a more accurate way. Finally, the present work is also characterized by detailed building examples which illustrate all three design options of the method in contrast to almost all the above design methods (Kawashima and Aizawa 1986; Ballio and Castiglioni 1994; Tiwari and Gupta 2000; Kunnath and Chai 2004; Lu and Wei 2008; Teran-Gilmore and Bahema-Arredondo 2008; Malhotra 2002; Bozorgnia and Bertero 2004; Panyakapo 2004), which emphasize their method and present very simple one-storey examples or (mainly) no building examples at all.

2. HYSTERETIC MODELS THAT INCORPORATE STRENGTH AND STIFFNESS DEGRADATION

Several hysteretic models have been proposed in the literature. Some of them have hysteresis rules that account for stiffness degradation by modifying the path by which the reloading branch approaches the backbone curve, e.g., the peak oriented model (Clough and Johnston1966) or various ‘pinching’ models (Takeda et al. 1970). In addition, smooth hysteretic models have been developed that include a continuous change of stiffness due to yielding, and sharp changes due to unloading, e.g. the Bouc-Wen model (Wen 1976). The need to model both stiffness and strength degradation led to the development of more versatile models like those of Sivaselvan and Reinhorn (2000), which include rules for stiffness and strength degradation as well as pinching. Song and Pincheira (2000) developed a model that is capable of representing cyclic strength and stiffness degradation based on dissipated hysteretic energy. This is essentially a peak-oriented model that considers pinching based on degradation parameters. Erberik and Sucuoğlu (2004) and Sucuoğlu and Erberik (2004) developed low-cycle fatigue, hysteresis and damage models for deteriorating systems on the basis of test data and analysis. Ibarra et al. (2005) created a model in which four modes of cyclic deterioration are defined with respect to the backbone curve based on the hysteretic response of the component. This was improved later by Lignos and Krawinkler (2011). In addition, models which trace the collapse capacity of steel braced frames or moment-resisting frames subjected to earthquakes have been proposed by Lavan et al. (2009), Sivaselvan et al. (2009), Krishnan and Muto (2012), Jin and El-Tawil S.(2003) and Li and El-Tawil (2013). In the commercial computer program Ruaumoko (Carr 2006), stiffness and strength degradation can be taken into account, among others, through a linear function that depends on the inelastic cycles a member sustains. This model is described next and used in this work because of its simplicity and agreement with experiments.

Ruaumoko (Carr 2006) is a program that performs nonlinear dynamic analysis with the aid of the finite element method and the concept of concentrated plasticity. Bending moment M - axial force N interaction is modeled by an M-N curve, like the one shown by Fig. 2, which indicates the

formation of a plastic hinge at a member. Furthermore, it utilizes, among others, a material behavior model that takes into account strength degradation. To allow for strength deterioration, the yield levels in the interaction diagram, may be reduced as functions of load reversals from the backbone or spine curve of the hysteresis rule. More specifically, for the two dimensional (2D) case examined herein, the strength loss in each loading direction is governed by a deterioration parameter that scales the initial strength and is a linear function of the number of inelastic cycles. It must be noted that the cycles number is defined as the number of times the hysteresis rule leaves the post-yield back-bone or skeleton curve divided by 2 and this might be greater than the number of cycles of hysteresis, particularly if there has been a one sided ratchet-like behavior of the hysteresis. This parameter *f* is given by the equation

$$f = \frac{S_r - 1}{n_2 - n_1}(n - n_1) + 1 \tag{1}$$

where n is the number of cycles, n_1 is the cycle at which degradation begins, n_2 the cycle at which degradation stops and S_r the residual strength factor that multiplies the initial yield strength to produce the residual strength. It is assumed that the stiffness deteriorates so that the yield displacement remains constant. Typical values of n_1, n_2 and S_r can be 3, 55 and 0.55, respectively. For these values of the abovementioned parameters, f is equal to 0.96 when n is 8, according to Eq. (1).

This has been extended recently to allow for a tri-linear degradation of strength with cycle number. It must be noted that in Ruaumoko (Carr 2006) it is not possible to have complete elimination of strength. If any action (axial force or bending moment) has both positive and negative yield actions equal to zero, the action is assumed to be elastic. This means that the action has infinite yield strength. A 1% strength is close enough to zero for engineering purposes and this is the minimum value permitted for S_r.

Finally, the model used herein does not incorporate the effect of softening per inelastic cycle of the moment - rotation hysteretic behavior of steel beams and columns. In contrary, other models as the Ibarra et al. (2005) model, take into account this phenomenon, which seems to be crucial in collapse assessment of structures. This issue is addressed by Ibarra and Krawinkler (2011), where an important influence on collapse capacity is reported when the post-capping slope of the backbone curve of the system is relatively flat (i.e. the system is more ductile). It is also observed that the collapse capacity may be reduced up to 20–30% when the post-capping stiffness, a_c, is decreased from -0.10 to -0.30.

For the calibration of the above material model of Ruaumoko 2D (Carr 2006), results from experiments performed by Ricles et al. (2000) were used. These experimental studies focused on the cyclic inelastic performance of full-scale welded unreinforced flange moment connection specimens. The experiment C2 of these studies was simulated by Ruaumoko 2D (Carr 2006) and the moment-rotation curves of the right beam of the connection were evaluated. The experimental curve is shown in Fig. 1, together with the one simulated by Ruaumoko 2D (Carr 2006). The agreement between the experimental and the numerical curves is considered to be satisfactory.

Parameters n_1, n_2 and S_r can be affected by the geometric and material characteristics of a steel cross section, but a parametric study to highlight this effect has not been conducted in this work. The main scope of this paper is to develop a new design method based on the proposed damage index and a damage scale for performance based design, so an assumption that all sections deteriorate in the same manner as the calibrated one has been made. This probably has an influence to the regression formulae discussed in the next section, but this influence is not much. On the other hand, that does not change the main philosophy of the proposed design method. Herein, the general rules of the method are presented and thus it is possible for a designer to make other assumptions. For example, one can take into account the impact of section properties on the degradation models or use more advanced deteriorating models.

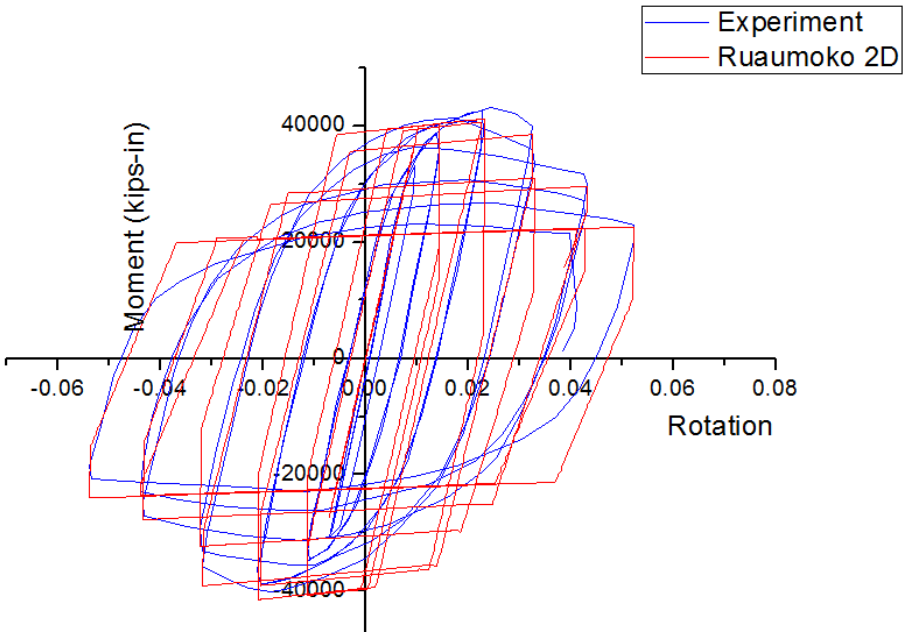

Figure 1. Moment-rotation hysteresis loops as obtained experimentally and analytically.

3. THE DAMAGE INDEX

In this section a damage index for steel members recently proposed by the authors (Kamaris et al. 2013) and used in this work because of its merits is briefly described for reasons of completeness. This damage index is defined at a section of a structural member by the equation (Kamaris et al. 2013)

$$D_S = \frac{c}{d} = \frac{\sqrt{(M_S - M_A)^2 + (N_S - N_A)^2}}{\sqrt{(M_B - M_A)^2 + (N_B - N_A)^2}} \tag{2}$$

In the above, the bending moments M_A, M_S and M_B and the axial forces N_A, N_S and N_B as well as the distances c and d are those shown in the bending moment M - axial force N interaction diagram of Fig. 2 for a plane beam-column element. Thus, this damage index takes into account the interaction between the bending moment M_S and axial force N_S acting at the specific section at a time instant during the loading history.

Figure 2 depicts a lower bound damage curve, the limit between elastic and inelastic material behavior and an upper bound damage curve, the limit between inelastic behavior and complete failure. Thus, damage at the former curve is zero, while at the latter curve is one. Equation (2) is based on the assumption that damage evolution varies linearly between the above two damage bounds. Points (M_A, N_A) and (M_B, N_B), can be found by drawing a line that connects point (M_S, N_S) to the origin of the axes. The intersection of the lower and upper bound damage curves to the above line determines the abovementioned points.

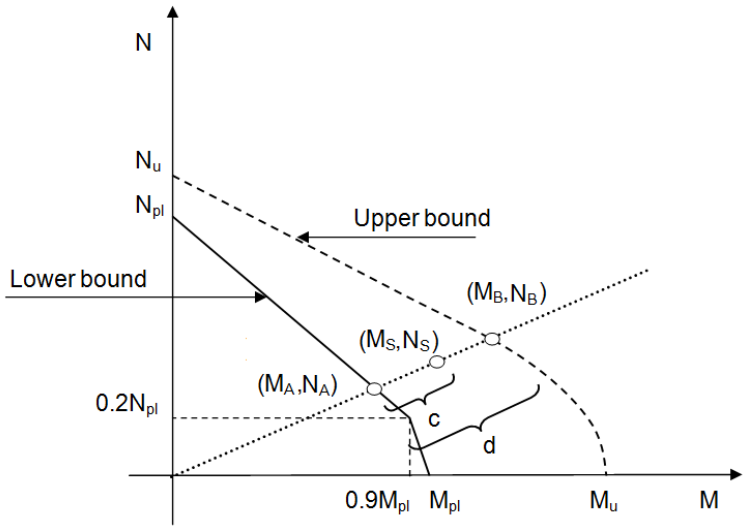

Figure 2. Bending moment-axial force interaction diagram and definition parameters of proposed damage index.

The lower bound curve of Fig. 2 is the one found in finite element programs of concentrated plasticity and indicates the formation of a plastic hinge at a member. In Ruaumoko (Carr 2006) program, used herein, the lower bound curve is described as

$$\frac{0.88M}{f\cdot M_{pl}}+\frac{N}{f\cdot N_{pl}}=1 \quad for \quad \mathrm{M}\le 0.9M_{pl} \quad and \quad N\le 0.2N_{pl}$$

$$\frac{M-M_{pl}}{f\cdot M_{pl}}+\frac{N}{f\cdot N_{pl}}=1 \quad for \quad \mathrm{M}> 0.9M_{pl} \quad and \quad N> 0.2N_{pl} \tag{3}$$

where N_{pl} and M_{pl} are given by the expressions

$$M_{pl}=f_y W_{pl}, \quad N_{pl}=f_y A \tag{4}$$

with f_y being the yield stress of steel, W_{pl} the section plastic modulus and A the sectional area.

The upper bound curve of Fig. 2 has a similar form with the *M-N* interaction formula given in EC3 (2010) provisions, with the hardening effect not taken into account, i.e., with $\sigma_u=\sigma_y$ or equivalently, $N_u=N_y$. Thus this curve can be expressed as

$$\frac{M}{f\cdot M_u}+\left(\frac{N}{f\cdot N_u}\right)^2=1 \tag{5}$$

where N_u and M_u are the ultimate axial force and bending moment, respectively, which cause failure of the section and are equal to

$$M_u=f_u W_{pl}, \quad N_u=f_u A \tag{6}$$

with f_u being the ultimate stress of steel. The factor f is the scale factor of Eq. (1) that is used so as phenomena of strength and stiffness degradation to be taken into account.

The increase of damage related to strength reduction due to low-cycle fatigue is taken into account by following the idea of Sucuoğlu and Erberik (2004) and results of extensive parametric studies of the authors as described in (Kamaris et al. 2013). This increase of damage ΔD_s can be computed by the empirical expression

$$\Delta D_s = 0.56 \cdot n^{0.292} \cdot D_s^{0.914} \tag{7}$$

where D_s is the damage index of Eq. (2) at that loading cycle.

Consequently, for a combination of moment M_S and axial force N_S computed at a member section, one can easily evaluate the damage index there by using Eqs (2) and (7) at each time step of a nonlinear dynamic analysis. The calculation of *M*-*N* pairs is conducted with the aid of the Ruaumoko 2D finite element program (Carr 2006). In this program, material nonlinearities are taken into account through a bilinear moment-rotation model, that incorporates strength and stiffness degradation in the framework of concentrated plasticity (plastic hinge model), while, geometrical nonlinearities are modeled by including large displacement effects. The computation of the damage index is done with the aid of a computer program in FORTRAN constructed by the authors.

The above damage index, as described in (Kamaris et al. 2013), is calibrated against experimental results and proves to be better than many of the most well known damage indices in the literature.

4. ESTABLISHMENT OF DAMAGE PERFORMANCE LEVELS

Damage is used here as a design criterion. Thus, the designer, in addition to a method for determining damage, also needs a scale of damage in order to decide which level of damage is acceptable or desirable for his design. Many damage scales can be proposed in order to select desired damage levels associated with the strength degradation and capacity of a structure to resist further loadings. Table 1 has been constructed on the basis of available data in the literature associated mainly with steel frames and provides three performance levels (IO = Immediate Occupancy, LS = Life Safety and CP = Collapse Prevention) associated with modern performance-based seismic design with the corresponding limit response values (performance objectives) in terms of IDR = interstorey drift ratio, θ_{pl} = plastic rotation at member end, μ_θ = local ductility and *d* = damage. The relevant references are also shown in Table 1. At this point one should mention that the damage limit values of the various references, correspond to different definitions of damage indices and hence they should be treated with caution.

In this section, new damage scales for plane steel moment resisting frames for the aforementioned three performance levels are constructed on the basis of extensive parametric studies involving a large number of frames and seismic motions. More specifically, in the following subsections, the frames and seismic motions considered are described and the computational methodology used to establish these damage scales is presented in detail.

Table 1. *Performance levels and corresponding limit response values given by several authors*.

Performance Levels	IDR	θ_{pl}	μ_θ	Damage
IO	0.2% (Ghobarah 2004) 1-2% (Leelataviwat et al. 1999) 1.5% (SEAOC 1999) 0.6% (Grecea et al. 2002) 0.5% (Vasilopoulos and Beskos 2006) 0.7 % transient negligible permanent (FEMA-273 1997)	$\leq\theta_y$ (FEMA-273 1997)	2 (FEMA-273 1997)	10-20% (Ghobarah 2004) ≤5% (Vasilopoulos and Beskos 2006) 0.1-10% (ATC13 1985)
LS	0.4-1.0% (Ghobarah 2004) 2-3% (Leelataviwat et al. 1999) 3.2 % (SEAOC 1999) 1.5% (Vasilopoulos and Beskos 2006) 2.5 % transient 1% permanent (FEMA-273 1997, Grecea et al. 2002)	$\leq 6\theta_y$ (FEMA-273 1997)	7 (FEMA-273 1997)	20-40% (Ghobarah 2004) ≤20% (Vasilopoulos and Beskos 2006) 10-30% (ATC13 1985)
CP	1.8% (Ghobarah 2004) 3-4% (Leelataviwat et al. 1999) 3.8% (SEAOC 1999) 3% (Vasilopoulos and Beskos 2006) 5 % transient 5% permanent (FEMA-273 1997)	$\leq 8\theta_y$ (FEMA-273 1997) ≤0.04 rad (Grecea et al. 2002)	9 (FEMA-273 1997)	40-80% (Ghobarah 2004) ≤50% (Vasilopoulos and Beskos 2006) 30-60% (ATC13 1985)

$\theta_y = W_{p/} f_y L_b / 6EI_b$, $\theta_y = W_{p/} f_y L_c \left(1 - N / N_y\right) / 6EI_c$ *for beams (b) and columns (c), respectively.*

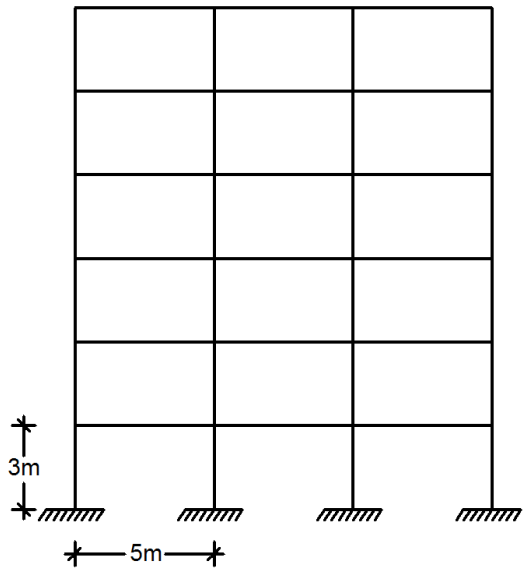

Figure 3. Geometry of a typical plane regular moment resisting steel frame.

4.1. Steel frames considered

A set of 36 plane steel moment resisting frames was employed for the parametric studies of this work. These frames are regular and orthogonal with storey heights and bay widths equal to 3 m and 5 m, respectively (Fig. 3). Furthermore, they have the following characteristics: number of stories n_s with values 3, 6, 9, 12, 15, and 20; number of bays n_b with values only 3 and 6 since it was found from preliminary studies that n_b has a rather small effect on a damage scale (Karavasilis et al. 2007, Karavasilis et al. 2008a). Various cases for the number of bays have been studied to examine the validity of this assumption and it was concluded that n_b is not important for the dynamic response of structures. A characteristic example of this study is presented herein, where damage of a three storey - three bay frame is compared to that of a three storey - six bay frame. The two frames were

subjected to the 40 ground motions of Table 3 and an incremental nonlinear dynamic analysis was performed in order to record the maximum damage of columns and beams, which are the variables used in the establishment of the proposed damage scale. The average maximum damage for the columns and beams of the first frame was 0.48 and 0.58 respectively. For the second frame these values were 0.50 and 0.55, indicating that there is a relative small difference in damage between the two frames, even though they correspond to different values of the parameter n_b. In addition, other researchers have presented similar conclusions as far as this parameter, which confirms that our choice not to examine this parameter is valid (Karavasilis et al. 2007, Karavasilis et al. 2008a). Capacity factors α with various values within practical limits were utilized. This capacity factor α of a frame is defined as

$$\alpha = M_{RC,1,av} / M_{RB,av} \tag{8}$$

where $M_{RC,1,av}$ is the average of the plastic moments of resistance of the columns of the first storey and $M_{RB,av}$ is the average of the plastic moments of resistance of the beams of all the stories of the frame. Gravity load on the beams is assumed to be equal to 27.5 KN/m (dead and live loads of floors), while the yield stress of steel was set equal to 235 MPa. The frames have been designed in accordance with the provisions of Eurocodes EC3 (2010) and EC8 (2008). The expected design ground motion was defined by the acceleration response spectrum of EC8 (2008) with a peak ground acceleration equal to 0.35 g and a soil class B. Data of the frames, including values for n_s, n_b, a, beam and column sections and first and second natural periods, are presented in Table 2 (Karavasilis et al. 2007). In that table, expressions of the form, e.g., 260–360(1–4) + 240–330(5–6) mean that the first four stories have columns with HEB260 sections and beams with IPE360 sections, whereas the next two higher stories have columns with HEB240 sections and beams with IPE330 sections.

Table 2. *Steel moment resisting frames considered in parametric studies*.

General data				Sections	Periods	
Frame	n_s	n_b	α	Columns: (HEB) & Beams: (IPE)	T_1(sec)	T_2(sec)
1	3	3	1.30	240-330(1-3)	0.73	0.26
2	3	3	1.60	260-330(1-3)	0.69	0.21
3	3	3	1.90	280-330(1-3)	0.65	0.19
4	3	6	1.30	240-330(1-3)	0.75	0.23
5	3	6	1.60	260-330(1-3)	0.70	0.21
6	3	6	1.90	280-330(1-3)	0.66	0.20
7	6	3	1.60	280-360(1-4)+260-330(5-6)	1.22	0.41
8	6	3	1.97	300-360(1-4)+280-330(5-6)	1.17	0.38
9	6	3	2.27	320-360(1-4)+300-330(5-6)	1.13	0.37
10	6	6	1.60	280-360(1-4)+260-330(5-6)	1.25	0.42
11	6	6	1.97	300-360(1-4)+280-330(5-6)	1.19	0.40
12	6	6	2.27	320-360(1-4)+300-330(5-6)	1.15	0.38
13	9	3	2.19	340-360(1)+340-400(2-5)+320-360(6-7)+300-330(8-9)	1.55	0.54
14	9	3	2.43	360-360(1)+360-400(2-5)+340-360(6-7)+320-330(8-9)	1.52	0.53
15	9	3	2.93	400-360(1)+400-400(2-5)+360-360(6-7)+340-330(8-9)	1.46	0.51
16	9	6	2.19	340-360(1)+340-400(2-5)+320-360(6-7)+300-330(8-9)	1.57	0.55
17	9	6	2.43	360-360(1)+360-400(2-5)+340-360(6-7)+320-330(8-9)	1.53	0.53
18	9	6	2.93	400-360(1)+400-400(2-5)+360-360(6-7)+340-330(8-9)	1.47	0.51
19	12	3	2.60	400-360(1)+400-400(2-3)+400-450(4-5)+360-400(6-7)+340-400(8-9)+340-360(10)+340-330(11-12)	1.90	0.66
20	12	3	3.00	450-360(1)+450-400(2-3)+450-450(4-5)+400-450(6-7)+360-400(8-9)+360-360(10)+360-330(11-12)	1.78	0.62
21	12	3	3.63	500-360(1)+500-400(2-3)+500-450(4-5)+450-450(6-7)+400-400(8-9)+400-360(10-11)+400-330(12)	1.72	0.60
22	12	6	2.60	400-360(1)+400-400(2-3)+400-450(4-5)+360-400(6-7)+340-400(8-9)+340-360(10)+340-330(11-12)	1.90	0.67

Table 2. *Continued.*

General data				Sections	Periods	
Frame	n_s	n_b	α	Columns: (HEB) & Beams: (IPE)	T_1(sec)	T_2(sec)
23	12	6	3.00	450-360(1)+450-400(2-3)+450-450(4-5)+400-450(6-7)+360-400(8-9)+360-360(10)+360-330(11-12)	1.78	0.63
24	12	6	3.63	500-360(1)+500-400(2-3)+500-450(4-5)+450-450(6-7)+400-400(8-9)+400-360(10-11)+400-330(12)	1.72	0.61
25	15	3	3.87	500-300(1)+500-400(2-3)+500-450(4-5)+450-400(6-7)+400-400(8-12)+400-360(13-14)+400-330(15)	2.29	0.78
26	15	3	4.49	550-300(1)+550-400(2-3)+550-450(4-5)+500-400(6-7)+450-400(8-12)+450-360(13-14)+450-330(15)	2.22	0.75
27	15	3	4.76	600-300(1)+600-400(2-3)+600-450(4-5)+550-450(6-7)+500-450(8-9)+500-400(10-12)+500-360(13-14)+500-330(15)	2.10	0.72
28	15	6	3.87	500-300(1)+500-400(2-3)+500-450(4-5)+450-400(6-7)+400-400(8-12)+400-360(13-14)+400-330(15)	2.30	0.78
29	15	6	4.49	550-300(1)+550-400(2-3)+550-450(4-5)+500-400(6-7)+450-400(8-12)+450-360(13-14)+450-330(15)	2.21	0.75
30	15	6	4.76	600-300(1)+600-400(2-3)+600-450(4-5)+550-450(6-7)+500-450(8-9)+500-400(10-12)+500-360(13-14)+500-330(15)	2.10	0.72
31	20	3	4.54	600-300(1)+600-400(2-3)+600-450(4-5)+550-450(6-10)+500-450(11-13)+500-400(14-16)+450-400(17)+450-360(18-19)+450-330(20)	2.82	0.97
32	20	3	5.19	650-300(1)+650-400(2-3)+650-450(4-5)+600-450(6-10)+550-450(11-13)+550-400(14-16)+500-400(17)+500-360(18-19)+500-330(20)	2.76	0.94
33	20	3	5.90	700-300(1)+700-360(2)+700-400(3)+700-450(4-5)+650-450(6-10)+600-450(11-13)+600-400(14-16)+550-400(17)+550-360(18-19)+550-330(20)	2.73	0.93
34	20	6	4.54	600-300(1)+600-400(2-3)+600-450(4-5)+550-450(6-10)+500-450(11-13)+500-400(14-16)+450-400(17)+450-360(18-19)+450-330(20)	2.75	0.96
35	20	6	5.16	650-300(1)+650-400(2-3)+650-450(4-5)+600-450(6-10)+550-450(11-13)+550-400(14-16)+500-400(17)+500-360(18-19)+500-330(20)	2.70	0.93
36	20	6	5.90	700-300(1)+700-360(2)+700-400(3)+700-450(4-5)+650-450(6-10)+600-450(11-13)+600-400(14-16)+550-400(17)+550-360(18-19)+550-330(20)	2.67	0.92

4.2. Ground motions considered

In this work, a set of 40 physical ground motions, selected from the PEER (2012) ground motion database, have been employed for the nonlinear dynamic analyses of this study. The main criterion used for this selection is that only far-fault ground motions are contained in this set, i.e., motions recorded at a distance more than 15 km from the causative fault. Ground motions which are characterized by distinct pulses in their velocity and displacement time histories were excluded from this study. In addition, the motions were selected so that their mean spectrum to be as close as possible to the response spectrum of EC8 (2008).The date, the record name, the excitation component and the peak ground acceleration (PGA) of the motions considered here are shown in Table 3. Their elastic response spectra are portrayed in Fig. 4, where the median spectrum is shown by a thick line. In order to cover the whole deformation range from elastic behavior up to collapse, all the aforementioned ground motions were scaled appropriately, using as intensity measure the first-mode spectral acceleration $S_a(T_1)$ and performing an incremental dynamic analysis (Vamvatsikos and Cornell 2002).

Table 3. *Characteristics of ground motions used in parametric studies.*

No.	Date	Record Name	Comp.	Station Name	PGA (g)
1.	1992/04/25	Cape Mendocino	NS	89509 Eureka	0.154
2.	1992/04/25	Cape Mendocino	EW	89509 Eureka	0.178
3.	1980/06/09	Victoria, Mexico	N045	6604 Cerro Prieto	0.621
4.	1980/06/09	Victoria, Mexico	N135	6604 Cerro Prieto	0.587
5.	1992/04/25	Cape Mendocino	EW	89324 Rio Dell Overpass	0.385
6.	1992/04/25	Cape Mendocino	NS	89324 Rio Dell Overpass	0.549
7.	1978/08/13	Santa Barbara	N048	283 Santa Barbara Courthouse	0.203
8.	1978/08/13	Santa Barbara	N138	283 Santa Barbara Courthouse	0.102
9.	1992/06/28	Landers	NS	12149 Desert Hot Springs	0.171
10.	1992/06/28	Landers	NS	12149 Desert Hot Springs	0.154
11.	1979/08/06	Coyote Lake	N213	1377 San Juan Bautista	0.108
12.	1979/08/06	Coyote Lake	N303	1377 San Juan Bautista	0.107
13.	1994/01/17	Northridge	NS	90021 LA - N Westmoreland	0.361
14.	1994/01/17	Northridge	EW	90021 LA - N Westmoreland	0.401
15.	1986/07/08	N. Palm Springs	NS	12204 San Jacinto - Soboba	0.239
16.	1986/07/08	N. Palm Springs	EW	12204 San Jacinto - Soboba	0.250
17.	1970/09/12	Lytle Creek	N115	290 Wrightwood	0.162
18.	1970/09/12	Lytle Creek	N205	290 Wrightwood	0.200
19.	1989/10/18	Loma Prieta	NS	58065 Saratoga - Aloha Ave	0.324
20.	1989/10/18	Loma Prieta	EW	58065 Saratoga - Aloha Ave	0.512
21.	1992/06/28	Landers	NS	22170 Joshua Tree	0.284
22.	1992/06/28	Landers	EW	22170 Joshua Tree	0.274
23.	1976/09/15	Friuli, Italy	NS	8014 Forgaria Cornino	0.212
24.	1976/09/15	Friuli, Italy	EW	8014 Forgaria Cornino	0.260
25.	1992/06/28	Landers	N045	24577 Fort Irwin	0.114
26.	1989/10/22	Loma Prieta	EW	678 Golden Gate Bridge	0.233
27.	1994/01/17	Northridge	EW	24389 LA - Century City CC North	0.256
28.	1994/01/17	Northridge	EW	24538 Santa Monica City Hall	0.883
29.	1994/01/17	Northridge	N279	90013 Beverly Hills- 14145 Mulhol	0.516
30.	1994/01/17	Northridge	EW	24278 Castaic - Old Ridge Route	0.568
31.	1994/01/17	Northridge	NS	90018 Hollywood - Willoughby Ave	0.245
32.	1994/01/17	Northridge	EW	24303 LA - Hollywood Stor FF	0.231
33.	1994/01/17	Northridge	N070	17-90015 LA - Chalon Rd	0.225
34.	1994/01/17	Northridge	EW	24400 LA - Obregon Park	0.355
35.	1994/01/17	Northridge	NS	24157 LA - Baldwin Hills	0.168
36.	1994/01/17	Northridge	EW	127 Lake Hughes #9	0.165
37.	1994/01/17	Northridge	N177	90063 Glendale - Las Palmas	0.357
38.	1994/01/17	Northridge	N035	90014 Beverly Hills- 12520 Mulhol	0.617
39.	1994/01/17	Northridge	NS	90047 Playa Del Rey - Saran	0.136
40.	1994/01/17	Northridge	EW	24401 San Marino, SW Academy	0.116

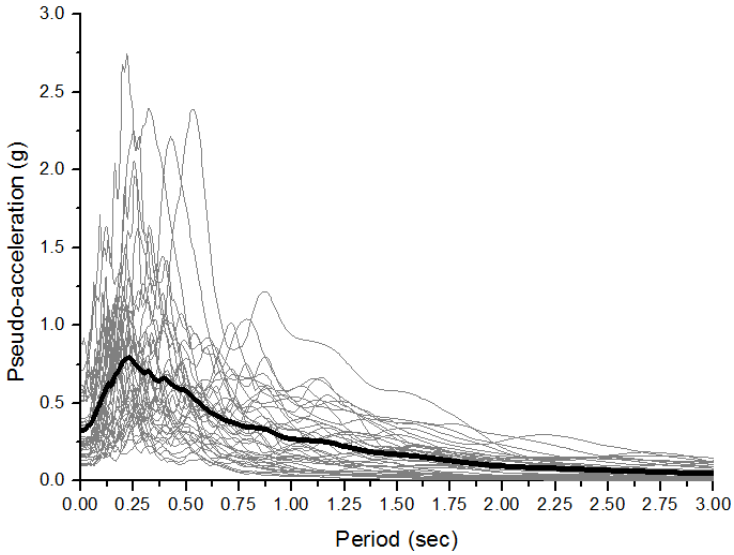

Figure 4. Response spectra of the ground motions considered in parametric studies.

4.3. Methodology for the damage scales determination

In the present work, an extensive parametric study was conducted for the 36 plane steel moment-resisting frames of Table 2, which were subjected to the 40 ground motions of Table 3 for the evaluation of the damage scales. The frames were analyzed with the program Ruaumoko 2D (Carr 2006) using the nonlinear dynamic analysis method. Thus, 23040 analyses (= 36 frames x 40 ground motions x 16 analyses on average for every frame) were conducted in this work. The mathematical models of the frames were based on centerline representations with inelastic material behavior modelled by means of bilinear (hysteretic) point plastic hinges with 3% hardening including cyclic strength and stiffness degradation. These models do not incorporate the strength and stiffness of the panel zone in connections, which were assumed to be rigid. Finally, diaphragm action was assumed at every floor due to the presence of the slab.

Maximum seismic response values, such as IDR's, plastic rotations, number of cycles and damage indices (computed on the basis of Eqs. (2) and (7)) for all the members of the frames and the whole range of seismic intensity for every motion (in a discrete manner) were carefully recorded to form a large response databank.

The Levenberg-Marquardt algorithm (MATLAB 1997) was adopted for the non-linear regression analysis of the results of the parametric studies, leading to two expressions, one for the columns and one for the beams, that give the maximum damage that is observed at a member, as a function of *IDR* (%) and the number of cycles *n*:

$$D_c = \frac{IDR^3}{132.903 + 4.695IDR^3}\left(1 - 0.162n + 1.887\sqrt{n}\right) \le 1.0 \tag{9}$$

$$D_b = \frac{IDR^3}{27.692 + 3.947IDR^3}\left(1 - 0.104n + 1.281\sqrt{n}\right) \le 1.0 \tag{10}$$

where D_c and D_b are the maximum column and beam damage, respectively, and n the number of cycles. Ignoring the effect of the number of cycles in the expressions for damage, the following relations can be adopted

$$D_c = \frac{IDR^3}{27.463 + 0.788IDR^3} \le 1.0 \tag{11}$$

$$D_b = \frac{IDR^3}{8.126 + 0.838 IDR^3} \leq 1.0 \tag{12}$$

Table 4 shows the basic statistical parameters for the proposed expressions.

Table 4. *Statistical parameters for the proposed expressions.*

Empirical expression	Correlation R^2	Standard deviation σ
Eq. (9)	0.74	0.304
Eq. (10)	0.91	0.226
Eq. (11)	0.72	0.339
Eq. (12)	0.87	0.272

Figure 5 shows the maximum damage of columns using the above empirical expressions (Eqs (9) and (11)), where for comparison reasons the 'exact' values from dynamic inelastic analyses are also provided. Although damage is evaluated herein deterministically, given the uncertainties associated with real seismic records, there is a scatter in the estimated seismic demands of a structure and, therefore, a statistical investigation is required. For this reason, the 16% and 84% confidence levels, corresponding to the median plus/minus one standard deviation, are also shown by heavy dashed lines (Vamvatsikos and Cornell 2002).

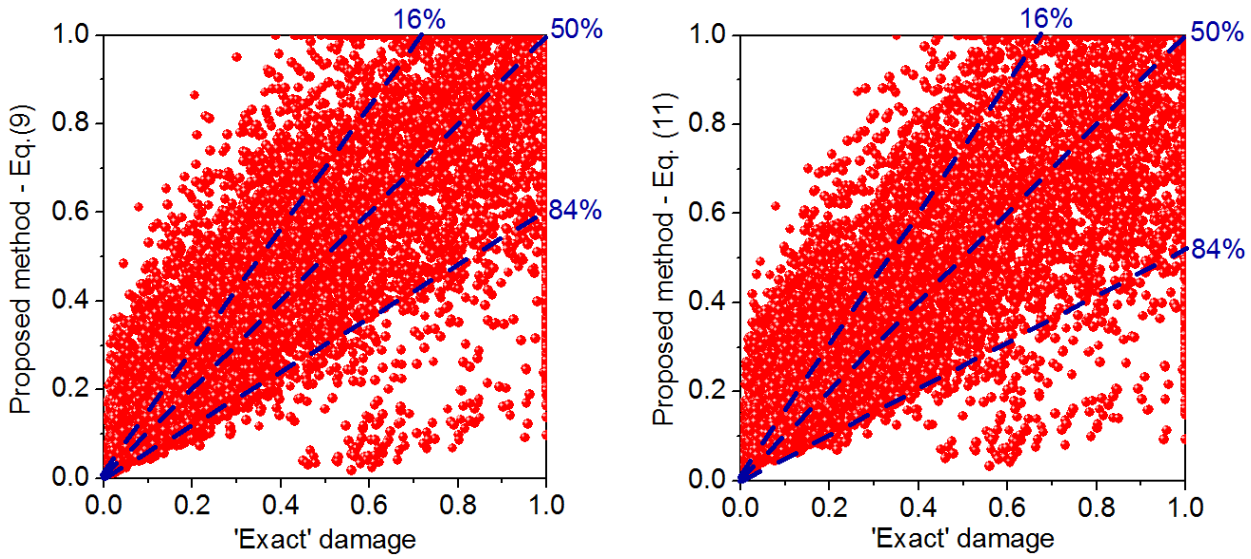

Figure 5. Maximum damage of columns: proposed method versus 'exact' values.

Similarly, Fig. 6 depicts the maximum damage of beams using the above empirical expressions, where for comparison reasons the 'exact' values from dynamic inelastic analyses are also given.

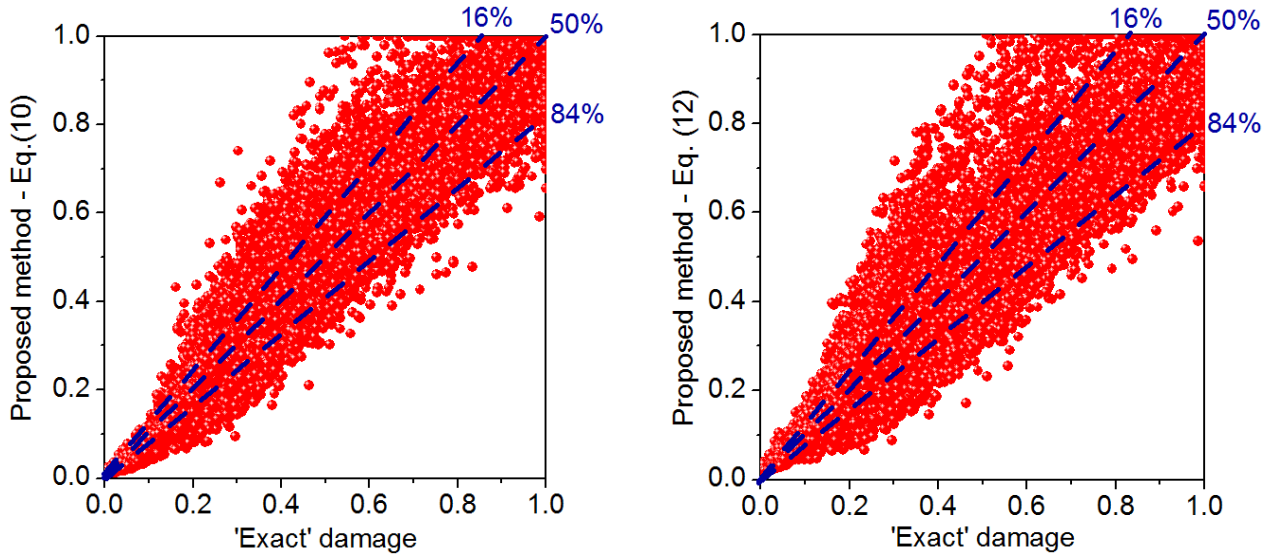

Figure 6. Maximum damage of beams: proposed method versus 'exact' values.

Additionally, Figure 7 shows the response databank 'exact' values and Eqs (9-12) for column and beam damage versus *IDR*.

Examining Figs 5 and 6, it is found that the dispersion is lower for the case of beam damage in comparison with the case of column damage. This scatter is probably due to the fact that the sample of data corresponding to columns is much smaller than that of beams. The formation of plastic hinges at columns is concentrated in column bases and thus the available data are less. In contrary, damage at beams is more uniformly distributed in the frames giving a better sample with less scatter. However, in both cases the accuracy is found to be satisfactory. Furthermore, it should be noted that examining the seismic analysis of structures, the scatter behavior of results is unavoidable; this has to do with the uncertainties associated with ground motions (Lam et al. 1998, Hatzigeorgiou 2010).

Examining Fig. 7, it is found that the number of cycles affects the structural damage and this influence can be considered using Eqs (9) and (10). The number of cycles can be directly related to the duration of a strong earthquake, where both the duration and the number of cycles of loading are positively correlated to structural damage. For example, the damage of steel moment resisting frames in the Northridge and Kobe earthquakes was attributed to low cycle fatigue (Raghunandan and Liel 2013). Additionally, the number of cycles should be taken into account examining multiple earthquakes (Hatzigeorgiou and Beskos 2009; Hatzigeorgiou 2010; Loulelis et al. 2012). This is also clearly shown in Fig. 8, which depicts the proposed method for medium to moderate damage (SP2 Performance Level according to SEAOC (1999), i.e., *IDR*=1.8%) and for moderate to major damage (SP3 Performance Level according to SEAOC (1999), i.e., *IDR*=3.2%).

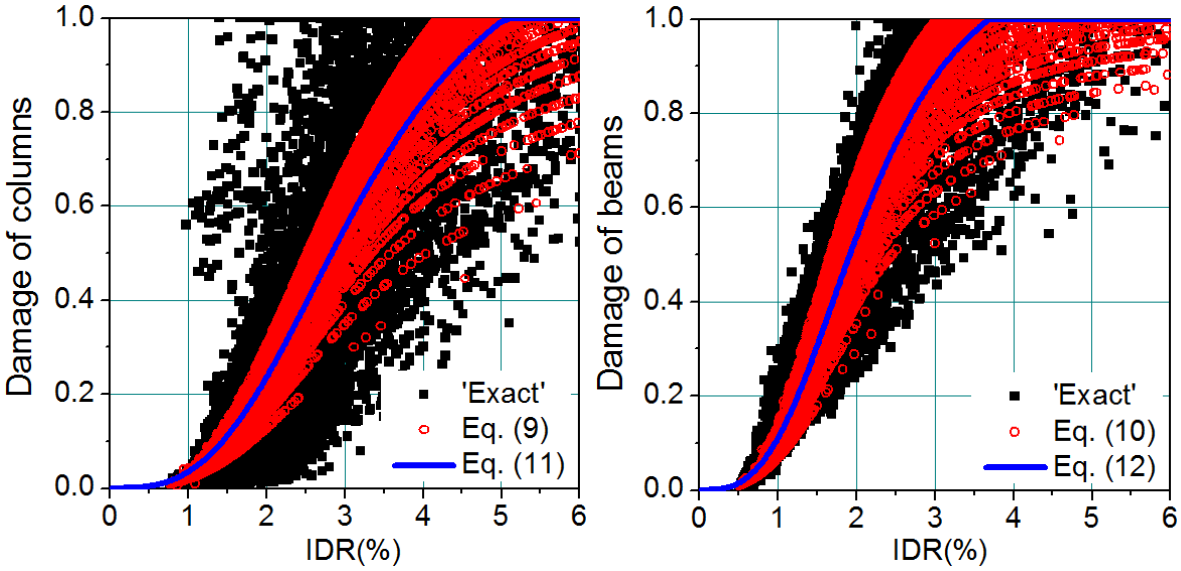

Figure 7. Damage of columns and beams versus *IDR*.

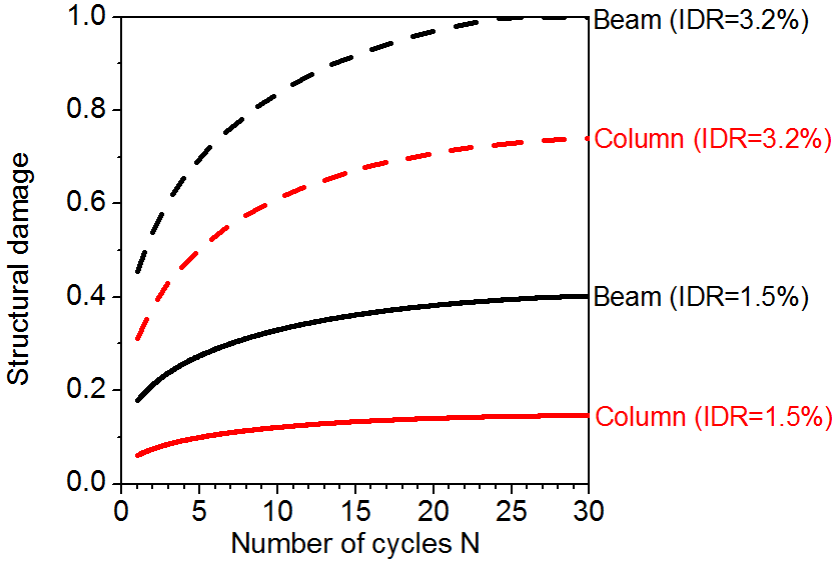

Figure 8. Damage of columns and beams versus number of cycles.

In case that, for simplicity reasons, the influence of number of cycles on damage is not considered, Eqs (11) and (12) can be used. Finally, considering or not the number of cycles, the aforementioned empirical expressions follow the general trend of 'exact' values from dynamic inelastic analyses and have the distinct sigmoid form (Fig. 7), of fragility curves which are used to estimate the damage probabilities of structures in earthquake-prone areas.

Using Eqs (11) and (12) as well as the values of the maximum IDR provided in FEMA-273 (1997), a damage scale for beams and columns for the performance levels of these guidelines, can be constructed. This damage scale is shown in Table 5. It is obvious that damage is very high in the CP performance level, especially for columns. This results from the fact that the corresponding value of *IDR* at the CP level, equal to 5%, seems to be extremely large and not conservative. For reasons of comparison, two additional damage scales are constructed using the mean values of IDR provided by Leelataviwat et al. (1999) and SEAOC (1995) and are given in Tables 6 and 7. It is observed now that because of lower values of IDR associated with these two scales, the corresponding damage values for columns for the CP level are also lower.

Table 5. *Damage scale proposed here for the performance levels of FEMA-273 (1997).*

Performance Levels	Maximum column damage	Maximum beam damage
IO	≤1%	≤4%
LS	≤39%	≤74%
CP	≤99%	100%

Table 6. *Damage scale proposed here for the performance levels of Leelataviwat et al. (1999).*

Performance Levels	Maximum column damage	Maximum beam damage
IO	≤11%	≤31%
LS	≤39%	≤74%
CP	≤70%	97%

Table 7. *Damage scale proposed here for the performance levels of SEAOC (1995).*

Performance Levels	Maximum column damage	Maximum beam damage
IO	≤1%	≤2%
LS	≤11%	≤31%
CP	≤39%	≤74%

5. DAMAGE CONTROLLED STEEL DESIGN

The application of the proposed Direct Damage Controlled Design (DDCD) method to the seismic design of plane moment-resisting framed steel structures is done with the aid of the Ruaumoko 2D (Carr 2006) program working in the time domain. In this program, material nonlinearities are taken into account by a stress-strain bilinear model including cyclic strength and stiffness degradation in the framework of concentrated plasticity (plastic hinge model), while geometrical nonlinearities are modeled by including large deflection effects.

The user has three design options at his disposal in connection with damage controlled steel design:

1. determine damage in any member or the whole of a designed structure under given seismic load
2. dimension a structure for given seismic load and desired level of damage
3. determine the maximum seismic load a designed structure can sustain in order to exhibit a desired level of damage.

The first option is the one usually done in current practice. The other two options are the ones which actually make the proposed design method a direct damage controlled one, with the second option providing the ability of easily applying capacity design (‘‘weak beams–strong columns’’). In all these options damage is evaluated by computing the proposed damage index, with the aid of Ruaumoko 2D (Carr 2006) program, by performing a non-linear dynamic analysis and using the Eqs (2) and (7) as described in Sec.3.

Sometimes, it is useful to provide an overall damage index that is representative of the damage

state of a part of a structure or the whole structure. The member damage indices must be combined in a rational manner to reflect both the severity of the member damage and the geometric distribution of damage within the overall structure. Various types of weighted-average procedures have been proposed for combining the member damage indices into an overall damage index. One well accepted such procedure computes the overall damage index D_o of a structure composed of m-members as in Powell and Allahabadi (1988)

$$D_o = \left(\sum_{i=1}^{m} D_i^2\right) \Big/ \left(\sum_{i=1}^{m} D_i\right) \tag{13}$$

where D_i is the local damage index defined at the section of a member.

6. EXAMPLES OF APPLICATION

In this section, a number of numerical examples concerning various frames are presented in order to illustrate the use of the proposed design method and demonstrate its advantages.

6.1. First design option for a three storey – three bay moment resisting steel frame

A plane three storey - three bay steel frame is examined in this example. The bay width is assumed equal to 5 m and the story height equal to 3 m, as shown in Fig. 9. Columns consist of standard HEB240 sections and beams of standard IPE330 sections, while the material properties correspond to structural steel grade S235. The frame is subjected to the vertical uniform load 27.5kN/m (dead and live loads of floors) plus seismic load. The frame has been designed in accordance with the provisions of EC3 (2010) and EC8 (2008) and its fundamental natural period is equal to 0.73 sec. The expected ground motion is defined by the elastic acceleration design spectrum of the EC8 (2008) seismic code, with peak ground acceleration equal to 0.35 g and a soil class B. The SAP2000 (2005) software package has been used for elastic analysis and steel design.

The above frame is subjected now to ground motion 3 of Table 3. The damage of all the members of the frame is determined and is depicted in Fig. 10(a). It is observed that, for this specific seismic motion, damage values are low everywhere. However, the damage pattern consists of concentrated damages only at the beam ends and the column bases to the ground indicating that for a higher enough seismic intensity the resulting plastic hinge mechanism will be of global collapse type, a result of satisfaction of the ‘‘weak beams–strong columns’’ requirement of capacity design. This is achieved by scaling up the above ground motion by a large scale factor (2.25) and the results are shown in Fig. 10(b).

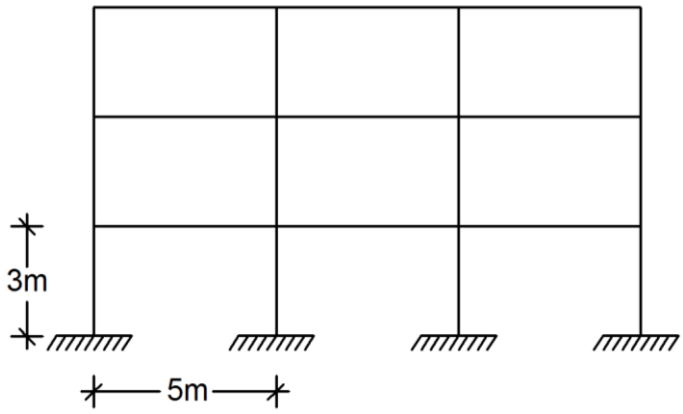

Figure 9. Geometry of the three storey frame of the example of sec. 6.1.

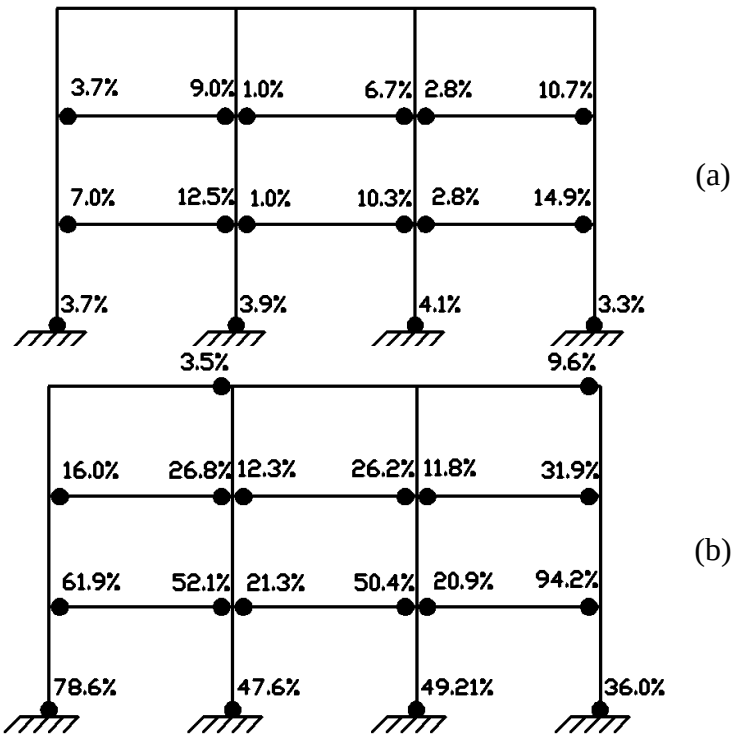

Figure 10. Damage indices in members of the frame of the example of Sec. 6.1: (a) for ground motion 3; (b) for scaled up ground motion 3.

6.2. Second design option for a three storey – three bay moment resisting steel frame

A plane three storey - three bay steel frame with geometry shown in Fig. 9 is examined in this example. Columns consist of standard HEB sections, while beams of standard IPE sections. Gravity load on the beams of the frame is assumed equal to 27.5 kN/m (dead and live loads of floors), while the yield strength of the material is set equal to 235 MPa. This frame should be dimensioned so as to satisfy the damage requirements of the second performance level (LS). Thus, a level of damage of 74% and 39% for the beams and the columns, respectively, is selected in agreement with the limits of Table 5 or based on Eqs (11) and (12) using the values of the maximum IDR provided in FEMA-273 (1997). It is also accepted that the columns of the first floor could develop plastic hinges at their bases. For the dynamic analysis of the frame, 8 semi-artificial accelerograms compatible with the EC8 (2008) spectrum were generated via a deterministic approach (Karabalis 1992) from 8 real ground motions of Table 3 to represent the design basis earthquakes (DBE). The response spectra of these motions, in comparison with the design spectrum of EC8 (2008), are depicted in Fig. 11. Thus, the performance objective of the design is LS under the DBE.

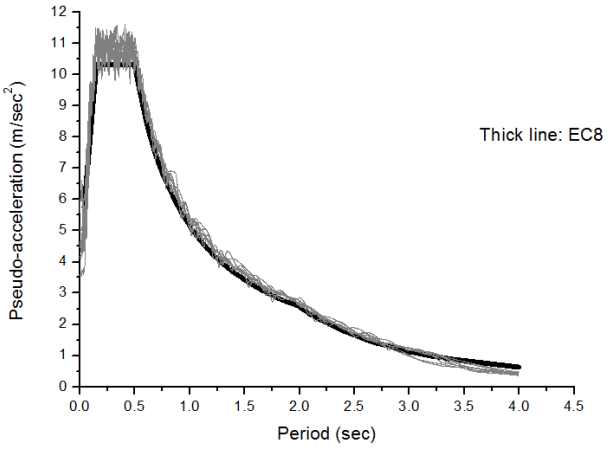

Figure 11. Response spectra of the ground motions used in the example of sec. 6.2.

The most appropriate sections were found to be IPE300 for the beams and HEB200 for the columns giving maximum damage values of 62.3% and 36.1% for the beams and the columns, respectively, for the case of the fourth accelerogram, as shown in Fig. 12. The values of damage computed are smaller than but close to the desired level of damage, thus the design is successful. The proposed method yielded in a structure of total weight of 4.1 tones and is more economical than the one by using the EC3 (2010) and EC8.(2008) codes, resulting in HEB240 and IPE330 sections for the columns and beams, respectively and total weight of 5.2 tones. The proposed design gives median values for IDR 2.2%, 2.0% and 1.1% for the first, second and third floor, respectively, which are in accordance with the LS performance level of FEMA-273 (1997), used for this design example and the construction of the damage scale. For the design based on the EC3 (2010) and EC8.(2008) codes the corresponding IDR values are 1.5%, 1.4% and 1.0% for the first, second and third floor, which are again within the limits of the LS performance level of FEMA-273 (1997). Furthermore, the proposed method is more exact because an inelastic dynamic analysis has been used. It is also apparent that the capacity design has been successfully implemented, because concentrated damage is formed only at the beams and at the base of the columns of the first floor, having weak-beam-strong-column ratios in the range of 1.1-2.0. It is observed that there is not plastic hinging in the columns of the frames, because an iterative procedure was followed, increasing the columns' sections in order that plastic hinges to be formed only at the column bases. Probably, if the finite dimensions of the panel zone have not been neglected, the results would have been different (SAC 2000, NIST 2010).

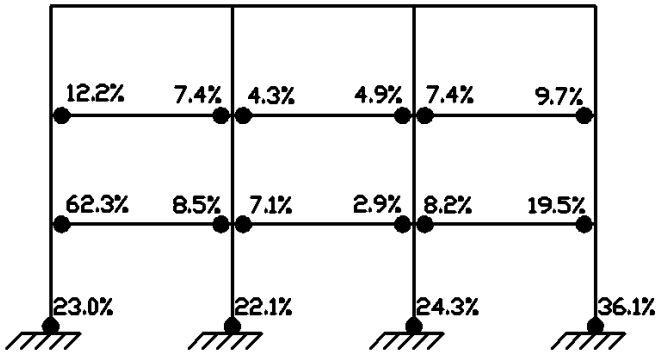

Figure 12. Distribution of damage in the frame of the example of Sec. 6.2 for the first excitation.

6.3. Second design option for a six storey – three bay moment resisting steel frame

In the following, a plane six storey - three bay steel frame with geometry as shown in Fig. 3 is examined here. Columns consist of standard HEB sections, while beams of standard IPE sections. Gravity load on the beams of the frame is assumed equal to 27.5 kN/m, while the yield strength of the material is set equal to 235 MPa. This frame should be dimensioned so as to satisfy the damage requirements of three performance levels. It is assumed that immediate occupancy (IO) under the frequently occurred earthquake (FOE), Life Safety (LS) under the Design Basis Earthquake (DBE) and Collapse Prevention (CP) under the Maximum Considered Earthquake (MCE) are the appropriate performance objectives for seismic design. The FOE, DBE and MCE are expressed through pseudo-acceleration design spectra of EC8 (2008) which have peak ground acceleration under DBE (PGA_{DBE}) equal to 0.35g. The peak ground accelerations under the FOE and the MCE, are expressed as functions of PGA_{DBE} and they are equal to 0.3 x PGA_{DBE} and 1.5 x PGA_{DBE}, respectively. In order to perform the dynamic analyses of the frame, 8 semi-artificial accelerograms compatible with the spectrum corresponding to each performance level were generated as before to represent the three different earthquakes. Thus, a level of damage that is in agreement with the limits of Table 5 is selected for the beams and the columns. The same limits can be computed by the Eqs (11) and (12) using the values of the maximum IDR provided in FEMA-273 (1997).

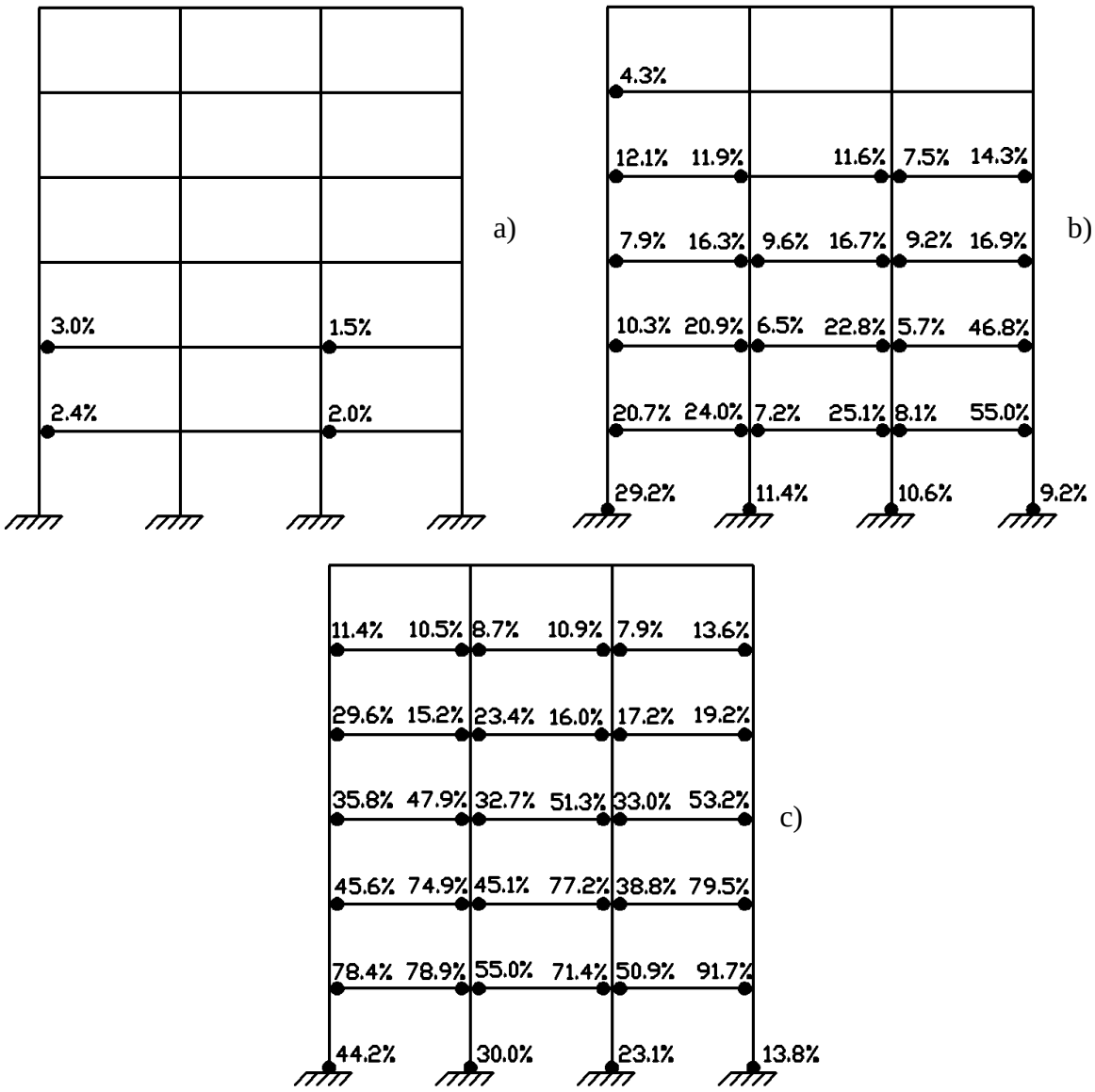

Figure 13. Distribution of damage in the frame of the example of Sec. 6.3:
a) First performance objective; b) Second performance objective; c) Third performance objective.

For the first performance objective, the most appropriate sections were found to be (HEB260-IPE330) for the first storey and (HEB240-IPE330) for the next five higher ones, giving maximum damage values of 3.0% and 0.0% for the beams and the columns, respectively, for the case of the eighth accelerogram, as shown in Fig. 13(a).

The sections IPE330 for the beams and HEB240 for the columns are selected for the second performance objective giving maximum damage values of 55.0% and 29.2% for the beams and the columns, respectively, for the case of the second accelerogram, as shown in Fig. 13(b).

Finally, the design for the third performance objective yields (HEB260-IPE360) for the first storey and (HEB260-IPE330) for the rest of the frame. This leads to maximum damage values of 91.7% and 44.2% for the beams and the columns, respectively, for the case of the third accelerogram, as shown in Fig. 13(c).

Thus, the most appropriate sections for this frame are those found for the last performance objective, yielding in a frame with total weight of 11.2 tones . This design is again more economical than the one by using the EC3 (2010) and EC8 (2008) codes and resulting in a frame with (HEB280-IPE360) for the first four stories and (HEB260-IPE330) for the next two higher ones and total weight of 12.1 tones. It also satisfies the capacity design as plastic hinges are formed only at the

beams and at the base of the columns of the first floor, giving weak-beam-strong-column ratios in the range of 1.25-3.0.

6.4. Third design option for a three storey – three bay moment resisting steel frame

The frame of the example of section 6.1 consisting of standard HEB240 sections for columns and standard IPE330 sections for beams is again considered here. This frame is subjected to the excitation of Cape Mendocino-1992 of Table 3 with PGA=0.154 g. For a desired level of damage defined by a maximum damage at columns and beams equal to 30% and 55%, respectively, one can determine the necessary value of PGA of the abovementioned accelerogram for the frame to reach this desired level of damage. The frame is analyzed with the aid of the program Ruaumoko 2D (Carr 2006) and a non-linear dynamic analysis is performed with increasing PGA values until values of damage less or equal to the desired ones are developed. It is found that for a value of PGA=0.8 g, the maximum values of damage at columns and beams are equal to 29.8% and 54.8%, respectively, indicating that this is the required seismic intensity to create the desired level of damage. For this seismic intensity, the maximum values of the number of inelastic cycles are found to be equal 14 for the columns and 17 for the beams, while the maximum IDR is 2%. Applying Eqs (11) and (12) the maximum values of damage at columns and beams, D_c and D_b respectively, are found to be 23.7% and 53.9% respectively. These values are very close to those computed by the nonlinear analysis. Application of the more accurate Eqs (9) and (10), which take into account the number of cycles, gives the values 27.2% and 60.9% for D_c and D_b, respectively, which are also very close to the computed ones. In addition, the estimation of the maximum damage at columns calculated by Eq (9) is much more accurate than the one given by Eq (11). Finally, the distribution of damage in this frame is shown in Fig. 14.

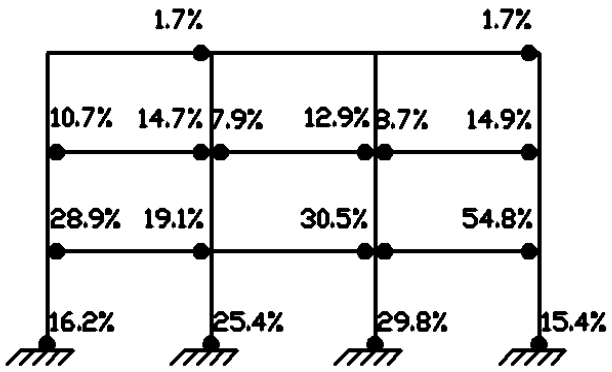

Figure 14. Distribution of damage in the frame of the example of Sec. 6.4.

7. CONCLUSIONS

On the basis of the preceding developments, the following conclusions can be stated:

1. A new method of seismic design of plane steel moment resisting frames subjected to ground motions, the Direct Damage Controlled Design (DDCD), has been developed, which can directly control damage in a structure locally or globally.
2. The method works with the aid of the finite element method incorporating material and geometric nonlinearities and working in the time domain. Programs like Ruaumoko or more commercial ones such as SAP2000, ETABS or Perform 3D can be successfully implemented for this type of analysis.
3. It uses a new damage index that accounts for the interaction between the axial force and the bending moment at a member section, incorporates cyclic strength and stiffness deterioration and accounts for the phenomenon of low-cycle fatigue.
4. It incorporates damage scales derived on the basis of extensive parametric studies, which are associated with three damage levels in a performance-based design framework.

5. This method allows the designer to either determine the damage level for a given structure under any given seismic load, or dimension a structure for given seismic load and desired level of damage, or determine the maximum seismic load a designed structure can sustain in order to exhibit a desired level of damage.
6. The method controls damage in a structure in a more direct and accurate manner than other methods and, at least for the examples considered here, leads to lighter sections than the ones obtained by using the seismic code provisions of EC3 and EC8.
7. Performance based design can be conducted as part of the second design option and the proposed damage scale. This is highlighted in the example of section 6.3 where a six storey - three bay steel frame was designed for three performance levels.

REFERENCES

Abbas M, Takewaki I.(2010) Characterization and modeling of near-fault pulse-like strong ground motion via damage-based critical excitation method, Structural Engineering and Mechanics 34 (6):755-778.

Abbas M.(2011) Damage-based design earthquake loads for single-degree-of-freedom inelastic structures, Journal of Structural Engineering of ASCE 137 (3):456-467.

Applied Technology Council (ATC13). (1985)Earthquake Damage Evaluation for California. Redwood City, California.

Aschheim A.(2002) Seismic design based on the yield displacement, Earthquake Spectra 18 (4):581-600.

Ballio G, Castiglioni CA.(1994) An approach to the seismic design of steel structures based on cumulative damage criteria, Earthquake Engineering and Structural Dynamics 23:969-986.

Bozorgnia Y, Bertero VV.(2004) Damage spectrum and its applications to performance-based earthquake engineering, Proceedings of 13th World Conference on Earthquake Engineering, Vancouver B.C., Canada, August 1-6, Paper No 1497.

Carr AJ. RUAUMOKO-2D.(2006) Inelastic Time-History Analysis of Two-Dimensional Framed Structures, Department of Civil Engineering. University of Canterbury, New Zealand.

Chopra AK, Goel PK.(2001) Direct displacement-based design: Use of inelastic vs elastic design spectra, Earthquake Spectra 17 (1):47-63.

Clough RW, Johnston SB.(1966) Effects of stiffness degradation on earthquake ductility requirements. Proceedings of the Japan Earthquake Engineering Symposium, Tokyo, Japan.

Cosenza E, Manfredi G, Ramasco R.(1993) The use of damage functionals in earthquake engineering: a comparison between different methods, Earthquake Engineering and Structural Dynamics 22:855-868.

EC3.(2010) Design of Steel Structures – Part 1-1: General Rules and Rules for Buildings, EN 1993-1-1:2005, European Committee for Standardization (CEN), Brussels.

EC8.(2008) Design of structures for earthquake resistance, Part 1: General rules, seismic actions and rules for buildings, European Standard EN 1998-1:2004, European Committee for Standardization (CEN), Brussels.

Erberik A, Sucuoğlu H.(2004) Seismic energy dissipation in deteriorating systems through low-cycle fatigue. Earthquake Engineering and Structural Dynamics 33:49-67.

FEMA-273.(1997) Building Seismic Safety Council, NEHRP guidelines for the seismic rehabilitation of buildings. Federal Emergency Management Agency, Washington (DC).

Ghobarah A.(2004) On drift limits associated with different damage levels, Performance-Based Seismic Design Concepts and Implementation, Fajar P, Krawinkler H (Editors), PEER Report 2004/05, University of California, Berkeley, pp. 321-332.

Ghobarah A, Abou-Elfath H, Biddah A.(1999) Response-based damage assessment of structures, Earthquake Engineering and Structural Dynamics 28:79-104.

Ghobarah A, Safar M.(2010) A damage spectrum for performance-based design, Advances in Performance-Based Earthquake Engineering, Fardis MN (Editor), Springer Science, Berlin, pp. 193-201.

Grecea D, Dinu F, Dubina D.(2002) Performance criteria for MR steel frames in seismic zones, Proceedings of EUROSTEEL 2002 Conference, Coimbra, Portugal, Lamas A, Da Silva LS (Editors), Multicomp, Lisboa, pp. 1269-1278.

Hatzigeorgiou GD.(2010) Behaviour factors for nonlinear structures subjected to multiple near-fault earthquakes. Computers and Structures 88 (5-6):309-321.

Hatzigeorgiou GD, Beskos DE.(2007) Direct damage-controlled design of concrete structures, Journal of Structural Engineering of ASCE 133 (2):205-215.

Hatzigeorgiou GD, Beskos DE.(2009) Inelastic displacement ratios for SDOF structures subjected to repeated earthquakes. Engineering Structures 2009; 31 (11):2744-2755.

Ibarra LF, Krawinkler H.(2011) Variance of collapse capacity of SDOF systems under earthquake excitations. Earthquake Engineering and Structural Dynamics 40 (12):1299–1314.

Ibarra LF, Medina RA, Krawinkler H.(2005) Hysteretic models that incorporate strength and stiffness degradation. Earthquake Engineering and Structural Dynamics 34:1489-1511.

Jin J, El-Tawil S.(2003). Inelastic cyclic model for steel braces. Journal of Structural Engineering, ASCE 129 (5):548-557.

Kamaris GS, Hatzigeorgiou GD, Beskos DE.(2009) Direct damage controlled design of plane steel-moment resisting frames using static inelastic analysis. Journal of Mechanics of Materials and Structures 4:1375-1393.

Kamaris GS, Hatzigeorgiou GD, Beskos DE.(2013) A new damage index for plane steel frames exhibiting strength and stiffness degradation under seismic motion. Engineering Structures 46:727-736.

Karabalis DL, Cokkinides GJ, Rizos DC.(1992) Seismic Record Processing Program-Ver.1.03, Report of the College of Engineering, University of South Carolina, Columbia.

Karavasilis TL, Bazeos N, Beskos DE.(2007) Behavior factor for performance-based seismic design of plane steel moment resisting frames. Journal of Earthquake Engineering 11 (4):531-559.

Karavasilis TL, Bazeos N, Beskos DE.(2008) Drift and Ductility Estimates in Regular Steel MRF Subjected to Ordinary Ground Motions: A Design-Oriented Approach. Earthquake Spectra 24 (2):431-451.

Karavasilis TL, Bazeos N, Beskos DE.(2008) A hybrid force/displacement seismic design method for steel building frames. In CD ROM Proccedings of the 14th World Conference on Earthquake Engineering, Beijing, China, 12-17 October.

Kawashima K, Aizawa K.(1986) Earthquake response spectra taking account of number of response cycles, Earthquake Engineering and Structural Dynamics 14:185-197.

Krishnan S, Muto M. (2012) Mechanism of collapse of tall steel moment-frame buildings under earthquake excitation. Journal of Structural Engineering , ASCE 138(11): 1361-1387.

Kunnath SK, Chai YH.(2004) Cumulative damage-based inelastic cyclic demand spectrum, Earthquake Engineering and Structural Dynamics 33:499-520.

Lam N, Wilson J, Hutchinson G. (1998) The ductility reduction factor in the seismic design of buildings. Earthquake Engineering and Structural Dynamics 27: 749-769.

Lavan O, Sivaselvan MV, Reinhorn AM, Dargush GF. (2009). Progressive collapse analysis through strength degradation and fracture in the Mixed Lagrangian Formulation. Earthquake Engineering and Structural Dynamics 38(13): 1483-1504.

Leelataviwat S, Goel SC, Stojadinović B.(1999) Towards Performance-Based Seismic Design of Structures. Earthquake Spectra 15 (3):435-461.

Lignos DG, Krawinkler H.(2011) Deterioration Modeling of Steel Components in Support of Collapse Prediction of Steel Moment Frames under Earthquake Loading. Journal of Structural Engineering, ASCE 137:1291-1302.

Li H, and El-Tawil S. (2013) Collapse resistance mechanisms in steel frame buildings. In Proceedings of the 2013 Structures Congress, pp. 1-10, Pittsburgh, Pennsylvania, May 2-4, 2013.

Loulelis D, Hatzigeorgiou GD, Beskos DE.(2012) Moment resisting steel frames under repeated earthquakes. Earthquakes and Structures 3 (3):231-248.

Lu Y, Wei J.(2008) Damage-based inelastic response spectra for seismic design incorporating performance considerations, Soil Dynamics and Earthquake Engineering; 28:536-549.

Malhotra PK.(2002) Cyclic-demand spectrum, Earthquake Engineering and Structural Dynamics 31:1441-1457.

MATLAB.(1997) The language of technical computing, Version 5.0. The Mathworks Inc., Natick, Mass.

NIST.(2010) Evaluation of the FEMA P-695 Methodology for Quantification of Building Seismic Performance Factors. NIST GCR 10-917-8, National Institute of Standards and Technology.

Panyakapo P.(2004) Evaluation of site-dependent constant-damage design spectra for reinforced concrete structures, Earthquake Engineering and Structural Dynamics 33:1211-1231.

Panyakapo P.(2008) Seismic capacity diagram for damage based design, Proceedings of 14th World Conference on Earthquake Engineering, Beijing, China.

Park YJ, Ang AHS, Wen YK.(1987) Damage-limiting aseismic design of buildings, Earthquake Spectra 3 (1):1-26.

PEER(2012) Pacific earthquake engineering research centre. Strong ground motion database: http://peer.berkeley.edu/.

Powell GH, Allahabadi R.(1988) Seismic damage prediction by deterministic methods: concepts and procedures. Earthquake Engineering and Structural Dynamics 16:719-734.

Priestley MJN, Calvi GM and Kowalsky MJ.(2007) Displacement-Based Seismic Design of Structures. IUSS Press. Pavia, Italy.

Raghunandan M. and Liel AB.(2013) Effect of ground motion duration on earthquake-induced structural collapse. Structural Safety 41:119-133.

Ricles JM, Mao C, Lu L-W, Fisher JW.(2000) Development and Evaluation of Improved Details for Ductile Welded Unreinforced Flange Connections. ATLSS Report No: 00-04, Lehigh University, Bethlehem.

Safar M, Ghobarah A.(2008) Inelastic response spectrum for simplified deformation-based seismic vulnerability assessment, Journal of Earthquake Engineering 12:222-248.

SAC Joint Venture. (2000) Recommended seismic design criteria for new steel moment frame buildings. Rep. No. FEMA 350, Federal Emergency Management Agency, Washington, D.C.

SAP2000.(2005) Static and Dynamic Finite Element Analysis of Structures. Version 9.1.4. Computers and Structures Inc., Berkeley, California.

Sivaselvan MV, Reinhorn AM.(2000) Hysteretic models for deteriorating inelastic structures. Journal of Engineering Mechanics, ASCE 126:633-640.

Sivaselvan, MV, Lavan O, Dargush GF, Kurino H, Hyodo Y, Fukuda R, Reinhorn AM. (2009). Numerical collapse simulation of large-scale structural systems using an optimization-based algorithm. Earthquake Engineering & Structural Dynamics 38(5): 655-677.

Song J, Pincheira J.(2000) Spectral displacement demands of stiffness and strength degrading systems. Earthquake Spectra 16:817-851.

Structural Engineers Association of California (SEAOC).(1999) Recommended lateral force requirements and commentary ''Blue Book''. Structural Engineers Association of California, 7th Edition Sacramento. CA.

Structural Engineers Association of California (SEAOC).(1995) Vision 2000: Performance Based Seismic Engineering of Buildings, San Francisco.

Sucuoğlu H, Erberik A.(2004) Energy-based hysteresis and damage models for deteriorating systems. Earthquake Engineering and Structural Dynamics 33:69-88.

Sullivan TJ, Calvi GM, Priestley MJN, Kowalsky MJ.(2003) The limitations and performances of different displacement-based design methods, Journal of Earthquake Engineering 7 (1):201-241.

Takeda T, Sozen, MA, Nielson NN.(1970) Reinforced concrete response to simulated earthquakes. Journal of the Structural Division, ASCE 96:2557-2573.

Teran-Gilmore A, Bahema-Arredondo N.(2008) Cumulative ductility spectra for seismic design of ductile structures subjected to long duration motions: concept and theoretical background, Journal of Earthquake Engineering 12:152-172.

Tiwari AK, Gupta VK.(2000) Scaling of ductility and damage-based strength reduction factors for horizontal motions, Earthquake Engineering and Structural Dynamics 29:969-987.

Vamvatsikos D. Cornell CA.(2002) Incremental dynamic analysis. Earthquake Engineering Structural Dynamics 31:491-514.

Vasilopoulos AA, Beskos DE.(2006) Seismic design of plane steel frames using advanced methods of analysis. Soil Dynamics and Earthquake Engineering 26:1077-1100.

Wen YK.(1976) Method for random vibration of hysteretic systems. Journal of the Engineering Mechanics Division, ASCE 112:249-263.